JOURNAL OF GEOPHYSICAL RESEARCH, VOL. 113, E07009, doi:10.1029/2008JE003114, 2008

Mobile lid convection beneath Enceladus' south polar terrain

Amy C. Barr[1]

Received 12 February 2008; revised 3 April 2008; accepted 6 May 2008; published 19 July 2008.

[1] Enceladus' south polar region has a large heat flux, 55–110 mW m^{-2}, that is spatially associated with cryovolcanic and tectonic activity. Tidal dissipation and vigorous convection in the underlying ice shell are possible sources of heat, however, prior predictions of the heat flux carried by stagnant lid convection range from $F_{conv} \sim 15$ to 30 mW m^{-2}, too low to explain the observed heat flux. The high heat flux and increased cryovolcanic and tectonic activity suggest that near-surface ice in the region has become rheologically and mechanically weakened enough to permit convective plumes to reach close to the surface. If the yield strength of Enceladus' lithosphere is less than ~1–10 kPa, convection may instead occur in the "mobile lid" regime, which is characterized by large heat fluxes and large horizontal velocities in the near-surface ice. I show that model ice shells with effective surface viscosities between 10^{16} and 10^{17} Pa s and basal viscosities between 10^{13} and 10^{15} Pa s have convective heat fluxes comparable to that observed by Composite Infrared Spectrometer. If this style of convection is occurring, the south polar terrain should be spreading horizontally with $v \sim 1–10$ mm a^{-1} (where a is years) and should be resurfaced in ~0.1–10 Ma. On the basis of Cassini imaging data, the south polar terrain is ~0.5 Ma old, consistent with the mobile lid hypothesis. Maxwell viscoelastic tidal dissipation in such ice shells is not capable of generating enough heat to balance convective heat transport. However, tidal heat may also be generated in the near-surface along faults as suggested by Nimmo et al. (2007) and/or viscous dissipation within the ice shell may occur by other processes not accounted for by the canonical Maxwell dissipation model.

Citation: Barr, A. C. (2008), Mobile lid convection beneath Enceladus' south polar terrain, *J. Geophys. Res.*, *113*, E07009, doi:10.1029/2008JE003114.

1. Introduction

[2] Observations of Enceladus by the Cassini spacecraft indicate that this tiny satellite is geologically active, with plumes of water vapor, dust, and other materials erupting from a region centered near its south pole dubbed the "south polar terrain" (SPT) [*Porco et al.*, 2006; *Spencer et al.*, 2006]. Enceladus' plumes are spatially associated with a region of increased heat flux, with a total power output of 5.8 ± 1.9 GW spread over a region ~70,000 km^2 [*Porco et al.*, 2006; *Spencer et al.*, 2006]. The total power output corresponds to a heat flux of $F = 55$ to 110 mW m^{-2}. The Cassini Composite Infrared Spectrometer (CIRS) instrument measured brightness temperatures ~80–90 K near the centers of the tiger stripes, four quasi parallel features ~500 km long, centered near the south pole. The active region at the south pole is bounded by cycloidal arcs, with wedge-shaped regions of intense folding at their cusps [*Helfenstein et al.*, 2006]. The SPT has very few craters, and none larger than 1 km, suggesting a young surface age ~0.5 Ma [*Porco et al.*, 2006]. On Enceladus, the CIRS data provide a unique opportunity to observe the heat flux from the surface of an icy satellite at the time of active resurfacing. The heat flux estimates can be used to argue for or against certain types of convective behavior, can clarify the relationship between convection and resurfacing on Enceladus, and may provide insight into convective-driven resurfacing on other icy satellites.

[3] The activity in the SPT is likely driven by tidal dissipation within Enceladus. The high brightness temperatures along the tiger stripes led *Nimmo et al.* [2007] to suggest that shear heating due to cyclical strike-slip deformation along fault zones within the stripes could be a dominant source of heat generation in the SPT. Another possiblity is that Enceladus' ice shell is heated from within by tidal dissipation and is vigorously convecting [*Barr and McKinnon*, 2007; *Roberts and Nimmo*, 2008]. In such a scenario, the tiger stripes could represent passive spreading centers, or shear heating within the centers of the tiger stripes [*Nimmo et al.*, 2007] and underlying solid state convection could combine to create the large regional heat flux. If convective motions could reach close to the surface of Enceladus, convective heat transport and associated

[1]Department of Space Studies, Southwest Research Institute, Boulder, Colorado, USA.

0148-0227/08/2008JE003114$09.00

lithospheric spreading may provide a natural explanation for the region's high heat flux [*Barr and McKinnon*, 2007] and the convergent morphology at the SPT margins. Here, I explore the hypothesis that the SPT is a region on Enceladus where the surface ice has become locally rheologically and mechanically weakened permitting "mobile lid" convection.

[4] In a convecting planetary mantle, the heat flux and the potential for convective-driven lithospheric deformation are controlled in part by the ratio between the viscosity of the material (ice or rock) at the planet's cold surface (η_0) and the viscosity of the mantle at its warm base (η_1), $\Delta\eta = \eta_0/\eta_1$. A basic requirement for mobile lid convection is $\Delta\eta < \exp(4\ (n + 1))$ [*Solomatov*, 1995, 2004], where $n \sim 1-4$ is the rheological stress exponent, which implies mobile lid behavior can occur for $\Delta\eta \lesssim 10^4$ for $n = 1$. The predicted $\Delta\eta$ for the outer ice I shells of outer solar system satellites, however, is so large that convection in the outer ice I shells of icy satellites is expected to be confined beneath a thick lid of immobile, cold, and highly viscous material that does not participate in convection, called a "stagnant lid." The presence of the stagnant lid inhibits advective heat transport by preventing convective plumes from reaching close to the surface of the satellite and also inhibits convective-driven resurfacing because thermal buoyancy forces are too small to deform the overlaying high-viscosity lithosphere.

[5] Stagnant lid convection, however, does not seem to be compatible with the appearance of the surfaces of terrestrial planets like Venus and Earth (see, e.g., *Schubert et al.* [2001] for general discussion), nor with the surfaces of tidally flexed icy satellites such as Europa and Enceladus, all of which display a rich variety of surface features suggestive of convective-driven resurfacing [e.g., *Helfenstein et al.*, 2006; *Pappalardo et al.*, 1998; *Prockter et al.*, 2002]. On terrestrial planets, microscale and macroscale defects (cracks and faults) accommodate deformation and facilitate the creation of zones of weakness in the Earth's crust, which limits the effective viscosity of the lithosphere and permits and mobile lid behavior [*Kohlstedt et al.*, 1995; *Tackley*, 2000; *Bercovici*, 2003; *Solomatov*, 2004]. As illustrated in Figure 1, mobile lid convection is characterized by high heat fluxes, substantial horizontal velocities of surface materials, and elongated convection cells, behaviors that are reminiscent of plate tectonics [*Schubert et al.*, 2001]. Europa's ice shell can exhibit mobile lid behavior if the effective viscosity of its near-surface ice is limited by the finite yield strength of the lithosphere. Mobile lid convection is possible on Europa if its lithosphere has a yield strength less than 0.02 MPa [*Showman and Han*, 2005]. The upper limit on convective heat transport and the amount of tidal heating in a stagnant lid ice shell on Enceladus is a factor of $\sim$3–4 smaller than the heat flux observed by CIRS [*Roberts and Nimmo*, 2008] (see also section 2).

[6] To determine whether mobile lid convection can occur on Enceladus, and is consistent with the observed heat flux and morphology of the SPT, I perform numerical simulations of mobile lid convection to constrain the relationship between rheological properties of ice, physical properties of the ice shell, and convective behavior. For activity to persist over geologically long timescales, heat transported by convection must be balanced by tidal heat generated within Enceladus' floating ice shell. A standard Maxwell viscoelastic tidal dissipation model is used to compare tidal dissipation and convective heat transport in a mobile lid ice shell on Enceladus as a function of the shell's viscosity, physical, and mechanical properties. For mobile lid convection to occur, the ice shell on Enceladus must have a low effective yield strength, and the Rayleigh number of the ice shell must exceed a critical value. I evaluate these quantities using estimates of the yield stress of ice based on terrestrial analogs and studies of lithospheric deformation on Europa. If mobile lid convection is occurring within the SPT, regional lithospheric extension and/or spreading will resurface the region on a timescale controlled by the rheological properties of the near-surface ice. Regional spreading/extension must be balanced by lithospheric loss at the margins of the terrain. These geological consequences provide a means by which the mobile lid hypothesis can be tested using Cassini data.

2. A Limit to Convective Heat Transport in the Stagnant Lid Regime

[7] Enceladus is likely fully differentiated at present, with a rocky core of radius $\sim$150–160 km [*Schubert et al.*, 2007; *Barr and McKinnon*, 2007] (depending on the density of its rocky component), and an outer ice I shell between 80 to 100 km thick. It is not known whether Enceladus has a global subsurface ocean, however, the activity in the south polar region would seem to require tidal strains of the magnitude available only to an ice shell decoupled from the rocky core [*Nimmo et al.*, 2007; *Roberts and Nimmo*, 2008]. A floating outer ice I shell on Enceladus would be heated largely from within by tidal dissipation, which may occur as a result of viscous dissipation due to daily tidal deformation [e.g., *Ojakangas and Stevenson*, 1989] and/or strike-slip motion along shallow faults [*Nimmo et al.*, 2007]. Tidal dissipation within Enceladus' rocky core is expected to be extremely small [*Roberts and Nimmo*, 2008], and radiogenic heating currently provides only $O(1)$ mW m^{-2} to the global heat flux [*Schubert et al.*, 2007]. Therefore, the processes that create and transport the observed heat flux likely occur entirely within Enceladus' ice shell.

[8] At the low stresses associated with thermal buoyancy on a small satellite like Enceladus, deformation in solid water ice is likely accommodated by diffusion creep [*Moore*, 2006; *Barr and McKinnon*, 2007], which occurs by volume diffusion creep. The effective viscosity from volume diffusion is strongly dependent on temperature (T) [*Goodman et al.*, 1981; *Goldsby and Kohlstedt*, 2001]

$$\eta = \frac{R_G T d^2}{14 V_m D_{o,v}} \exp\left(\frac{Q_v^*}{R_G T}\right), \tag{1}$$

where R_G is the gas constant, $V_m = 1.95 \times 10^{-5}$ m^3 mol^{-1} is the molar volume, $D_{o,v} = 9.10 \times 10^{-4}$ m^2 s^{-1} is an estimate of the diffusion coefficient [*Goldsby and Kohlstedt*, 2001], and $Q_v^* = 59.4$ kJ mol^{-1} is the activation energy, and d is the ice grain size. On the basis of equation (1), the expected ratio between the viscosity at $T = T_b = 273$ K at the base of Enceladus' ice shell and $T = T_s = 70$ K is $\Delta\eta \sim 10^{32}$, which suggests that convection in Enceladus' outer ice I shell would be confined beneath a thick stagnant lid. Equation (1), however, does not adequately describe how extremely cold ice responds to an applied stress. Like any planetary

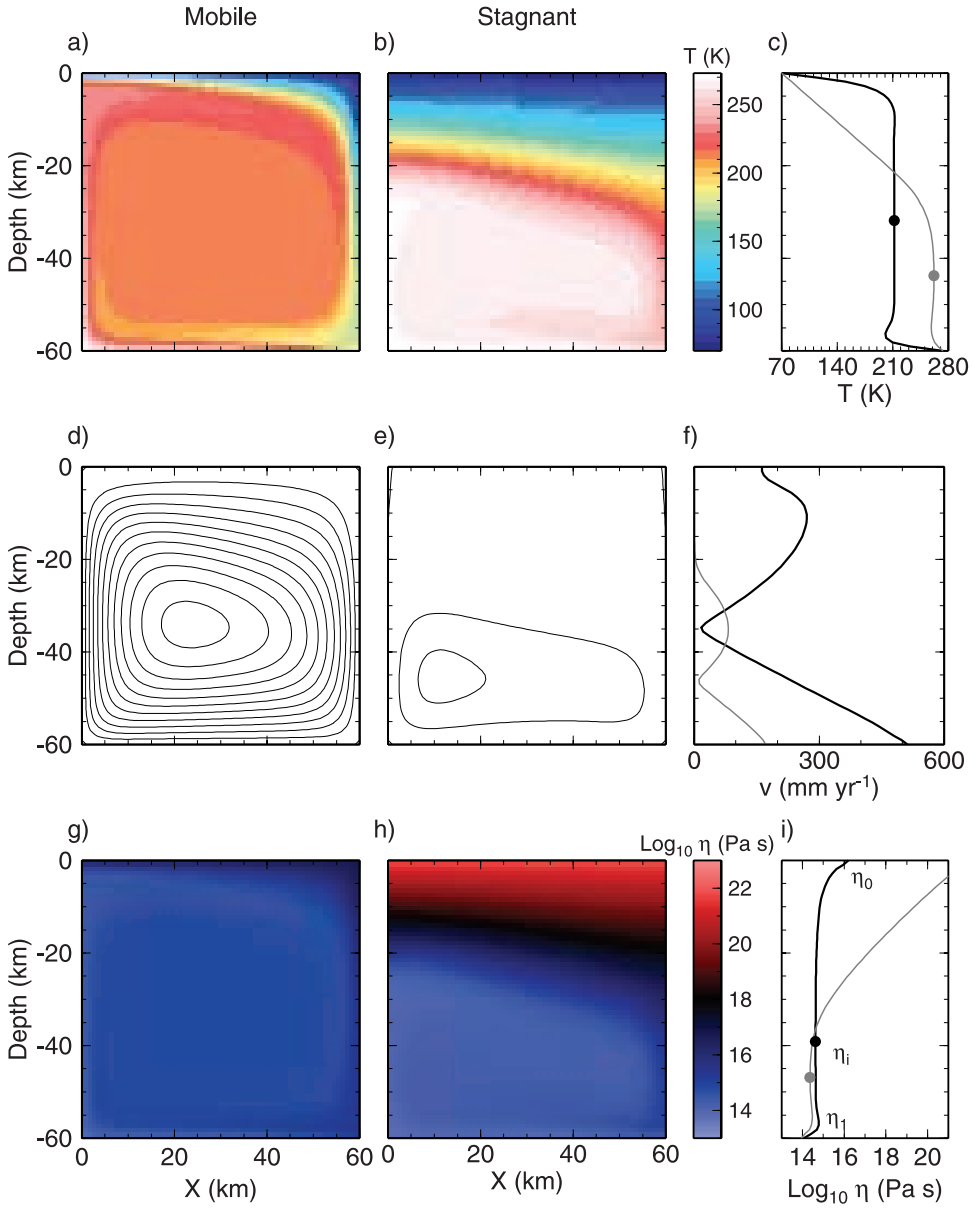

Figure 1. Comparison between convective temperature, flow, and viscosity fields for an ice shell with $Ra_1 = 10^7$, appropriate for Enceladus' ice shell with a basal ice viscosity $\eta_1 = 7 \times 10^{13}$ Pa s for (left) mobile lid convection with $\Delta\eta = 10^{2.5}$ and (middle) stagnant lid convection with $\Delta\eta = 10^8$. (a) In mobile lid convection, convective plumes rise close to the surface of the ice shell, permitting a large convective heat flux. In this case, F_{conv} = 110 mW m^{-2} (Nu = 14.35), compared to (b) the large $\Delta\eta$ case, where plumes are trapped beneath a thick stagnant lid and F_{conv} = 15 mW m^{-2} (Nu = 1.97). (c) The horizontally averaged temperature in the mobile lid case (black) is much lower than the stagnant lid case (gray). Dots on both lines indicate the locations of the characteristic temperatures in the convective interior T_i. Contours of stream function for the (d) mobile lid and (e) stagnant lid cases (f) and horizontally averaged velocity. Surface velocities are ~170 mma^{-1} (where a is years) in the stagnant lid case (black) whereas v ~0 at the surface for $\Delta\eta = 10^8$ (gray). Viscosity in the ice shell for the (g) mobile lid and (h) stagnant lid cases (i) and horizontally averaged viscosity as a function of depth for both cases. Dots on the viscosity profiles show the value of the characteristic viscosity in the convecting interior η_i and labels illustrate the effective surface viscosity η_0 and basal viscosity η_1. Although the viscosities in the convecting interior are comparable in both regimes, the strongly temperature-dependent viscosity in the stagnant lid case dictates high surface viscosities $\eta_0 \sim 10^{22}$ Pa s.

lithosphere, the cold near-surface ice in a convecting shell on Enceladus is expected to exhibit a brittle/elastic behavior, with viscous behavior dominating only at depth and in ice with temperatures close to the melting point. One way of mimicking the effects of a brittle lithosphere in a purely viscous convection model is to limit the viscosity of the near-surface ice, effectively decreasing $\Delta\eta$. This will be discussed in more detail in section 3.1.

[9] The heat flux out of a convecting ice shell is related to the thickness of the shell, (D), the thermal conductivity of the shell, (k), and the difference between the surface and basal temperature ($\Delta T = T_b - T_s$) as

$$F_{\mathrm{conv}} = \frac{k\Delta T}{D} Nu, \tag{2}$$

where $k = 2.27$ W m^{-1} K^{-1} is the thermal conductivity of water ice, Nu is the Nusselt number, which expresses the relative efficiency of convective heat transport over conduction alone (i.e., in a conductive ice shell, $Nu \equiv 1$). In a vigorously convecting, internally heated fluid with a strongly temperature-dependent viscosity, Nu is related to θ and the Rayleigh number (Ra), which expresses the vigor of convection [*Solomatov and Moresi*, 2000]

$$Nu = 0.53\theta^{-4/3} Ra_i^{1/3}, \tag{3}$$

where $\theta \approx Q_v^* \Delta T / R_G T_i^2$, and T_i is the temperature in the well-mixed convecting interior of the ice shell. In equation (3), Ra_i is the Rayleigh number of the ice shell evaluated at the viscosity in the convecting interior (see Figure 1), η_i,

$$Ra_i = \frac{\rho g \alpha \Delta T D^3}{\kappa \eta_i}, \tag{4}$$

where $\rho = 920$ kg m^{-3}, $g = 0.13$ m s^{-2} is the local acceleration of gravity within the ice shell ($g = 0.11$ m s^{-2} at the surface, and increases to 0.15 m s^{-2} at the base of the ice shell [*Barr and McKinnon*, 2007]), $\alpha = 1.56 \times 10^{-4}$ (T_b/250 K) = 1.7×10^{-4} K^{-1} is the coefficient of thermal expansion, and $\kappa = 1.47 \times 10^{-6}$ (250/T_b)^2 = 1.23×10^{-6} m^2 s^{-1} is the thermal diffusivity [*Kirk and Stevenson*, 1987].

[10] Equation (3) applies to basally and internally heated convection, but was developed to describe convection in a fluid driven by uniformly distributed internal heating and cooling from its upper surface [*Solomatov and Moresi*, 2000]. Enceladus' ice shell is heated from within by tidal dissipaiton, which is thought to occur because of viscous dissipation driven by diurnal tidal motion. Such heating is thought to be concentrated in regions of the ice shell with a low viscosity, and implicitly, a high temperature [*Tobie et al.*, 2003; *Showman and Han*, 2004]. Simulations of convection with viscosity-dependent tidal dissipation by *Tobie et al.* [2003] and *Showman and Han* [2004] show that tidal heating within the stagnant lid is negligible, and that temperature fluctuations driven by any heat deposited in the stagnant lid quickly diffuse away. Tidal dissipation, therefore, does not fundamentally alter the behavior or thickness of the stagnant lid. As a result, scalings for uniformly heated fluid layers (such as equation (3)) should provide a good approximation to the behavior of a tidally heated ice shell.

[11] Evaluating Nu in equation (2) using equations (3) and (4) gives an expression for F_{conv} that depends only on T_i and descriptive properties of ice

$$F_{\mathrm{conv}} = 0.53 \left(\frac{Q_v^*}{R_G T_i^2} \right)^{-4/3} \left(\frac{\rho g \alpha k^3}{\kappa \eta(T_i)} \right)^{1/3}. \tag{5}$$

Note that for vigorous convection in the stagnant lid regime, the convective heat flux does not depend on the thickness of the ice shell, D. Therefore, the upper limit on heat transfer is controlled simply by the rheology of the ice (through the activation energy and η_i). The convective heat flux is maximized when $T_i \sim T_b$, a state that is also required for long-term thermodynamic stability of Enceladus' ocean [*McKinnon and Barr*, 2008]. A lower limit on η_i can be obtained by evaluating the volume diffusion rheology at $T = T_b$ and $d \sim 0.1$ mm, a plausible lower limit for ice grain size in natural systems [*McKinnon*, 2006], which gives $\eta_1 = 6 \times 10^{13}$ Pa s. Using these parameters, the maximum heat flux from tidally or basally heated convection is $F_{\mathrm{conv}} \sim 20$ mW m^{-2}, a factor of $\sim$3–4 lower than the heat flux observed at the SPT. Relaxing the constraint on ice grain size to permit $\eta_1 = 10^{13}$ Pa s permits only a modest increase in F_{conv} to 33 mW m^{-2}, still less than the observed SPT value. *Roberts and Nimmo* [2008] have shown that tidal dissipation in an ice shell with the nominal volume diffusion rheology produces a heat flux from tides $F_{\mathrm{tidal}} < F_{\mathrm{conv}}$ and F_{tidal} much less than the regional heat flux observed by CIRS. This strongly suggests that processes other than a simple balance between convective and tidal heating in the stagnant lid regime are at work in the SPT.

3. Heat Transport in the Mobile Lid Regime

[12] To determine whether mobile lid convection can produce heat flows comparable to those observed in the SPT, it is necessary to perform numerical simulations of this style of convection to obtain a relationship between the Rayleigh number of the ice shell and the Nusselt number. I simulate Newtonian basally heated convection with a $\Delta\eta$ low enough for mobile lid behavior (the simplest mobile lid system) because a description of its behavior and implications for heat transport on icy satellites is lacking. I first describe the theoretical relationships between the rheology of the fluid, the Rayleigh number, and the convective heat flux in the stagnant and mobile lid regimes on the basis of the work of *Solomatov* [1995]. These theoretical relationships and numerical results are used to determine a relationship between convective heat flux, rheological properties of ice, and physical properties of Enceladus' ice shell. The scaling developed here represents a first step toward understanding mobile lid convection on icy satellites and can inform future studies of more complex mobile lid systems.

3.1. Background

[13] As its name implies, the mobile lid regime of convective behavior is characterized by large horizontal surface velocities of the convecting fluid, but also by large convective heat fluxes and relatively elongated convective cells (see *Schubert et al.* [2001] for general discussion). In

stagnant lid convection, near-surface material is completely immobile and convective plumes are trapped beneath the high-viscosity lid, which imposes a limit on convective heat transfer. The stagnant lid also suppresses the dynamic topography created by convective upwellings: the modest thermal buoyancy stresses associated with convection beneath the lid are not able to create uplift in the overlaying cold and viscous surface material. In basally heated stagnant lid convection, the natural wavelength of convective upwellings and downwellings is comparable to, or smaller than, the thickness of the convecting fluid layer. By contrast, convective plumes reach close to the surface in mobile lid convection, permitting high heat fluxes; the conductive boundary layer at the surface of the planet is extremely thin. In mobile lid convection, thermal buoyancy stresses are able to drive deformation in the near-surface material. The natural wavelength of convective upwellings in basally heated mobile lid convection can be very large, between 1 to 4 times the thickness of the fluid layer [*Ratcliff et al.*, 1997; *Kameyama and Ogawa*, 2000].

[14] Mobile lid convection has been most thoroughly characterized in the regime of parameter space appropriate for terrestrial planets because some of the behaviors in this regime are reminiscent of plate tectonics. Such studies are focused on determining why Earth is seemingly the only planet with plate tectonics at present; studying the criteria required for mobile lid convection and the motion of near-surface material clarifies the coupling between the behavior of the Earth's lithosphere and underlying mantle convection [see, e.g., *Moresi and Solomatov*, 1998; *Solomatov*, 2004]. Recently, mobile lid convection has been studied as a possible explanation for the variety of features on Europa's surface inferred to result from tidally driven convection in its ice shell. *Showman and Han* [2005] induced mobile lid behavior in Europa's ice shell by limiting the viscosity of its near surface ice to $\eta_{eff} \sim \sigma_Y/\dot{\varepsilon}_{II}$, where σ_Y is the yield stress of the ice, and $\dot{\varepsilon}_{II}$ is the second invariant of the strain rate tensor (a similar procedure has been used to model mobile lid behavior on Venus and the Earth [*Moresi and Solomatov*, 1998; *Solomatov*, 2004]). *Showman and Han* [2005] characterized the topography and overall fluid dynamical behavior of the shell as a function of yield stress. They find that periodic mobilization and foundering of Europa's near-surface icy crust can occur for $\sigma_Y \sim 0.01-0.06$ MPa, and continuous recycling of surface material (true mobile lid behavior) can occur for $\sigma_Y \sim 0.02$ MPa.

[15] Although the works described above shed light upon the behavior of mobile lid convection, they are almost exclusively focused on the formation of and deformation within the lid, and do not provide much insight into the relationship between convective heat flux and physical and rheological properties of the planetary mantle. Here, I use numerical simulations of convection with a low effective $\Delta\eta$ to constrain the relationship between *Ra* and *Nu* in the mobile lid regime, and to determine the conditions under which the heat flux from mobile lid convection is comparable to that observed by CIRS.

3.2. Scaling of Mobile Lid Convection

[16] In a convecting fluid layer heated from beneath, heat must be conducted across boundary layers at its warm base and cold upper surface. The thickness of each boundary layer is inversely proportional to the vigor of convection: when convection is extremely vigorous (for large *Ra*), plumes can transport heat close to the surface of the fluid, so the surface boundary layer is thin. In a fluid with a temperature-dependent viscosity, the thickness of each boundary layer is also proportional to $\theta = \ln(\Delta\eta)$, with large θ implying a thick conductive boundary layer (or stagnant lid) at the cold upper surface (see Figure 1).

[17] If the upper boundary layer has thickness $\delta_0 D$ and the bottom boundary layer $\delta_1 D$, the dimensionless heat flux, $Nu = F_{\text{conv}} (k\Delta T/D)^{-1}$ is related to the boundary layer widths as [*Solomatov*, 1995]

$$Nu \sim \frac{D}{(\delta_0 + \delta_1)}. \tag{6}$$

In the stagnant lid regime, $\delta_0 \sim D\theta^{4/3} Ra_i^{-1/3}$, and the bottom thermal boundary layer is thinner by a factor of $1/\theta$: $\delta_1 \sim \delta_0/\theta$ [*Solomatov*, 1995]. In stagnant lid convection, $\theta \gg 1$, which implies $\delta_0 \gg \delta_1$ in equation (6), so $Nu \sim D/\delta_0$. This gives rise to equation (3), where $Nu \sim \theta^{-4/3}\, Ra_i^{1/3}$.

[18] Similar to the stagnant lid regime, the *Ra*-*Nu* relationship in the mobile lid regime has the form [*Olson and Corcos*, 1980; *Moresi and Solomatov*, 1998]

$$Nu \sim Ra_i^{1/3}. \tag{7}$$

On Enceladus, the ice viscosity in the well-mixed convecting interior of the ice shell, η_i, and Rayleigh number, Ra_i, are not known a priori, so a scaling relationship involving these parameters is not useful for making predictions about its heat flux. A similar uncertainty regarding the properties of Venus' mantle was faced by *Moresi and Solomatov* [1998], who suggest a scaling of form

$$Nu = aRa_0^{1/3} \exp(\theta/b), \tag{8}$$

where a and b are empirical constants,

$$Ra_0 = \frac{\rho g \alpha \Delta T D^3}{\kappa \eta_0}, \tag{9}$$

and η_0 is the effective viscosity at the satellite's surface. If η_i is evaluated using the experimental result from constant viscosity convection, $\eta_i \approx \eta(\Delta T/2) \approx \eta_0 \exp(\theta/2)$ [e.g., *Booker*, 1976], this gives $b = 6$.

[19] To constrain a and b to obtain a relationship between the convective heat flux and descriptive properties of a Newtonian ice shell, I performed numerical simulations of convection in basally heated ice shells with $10^2 < \Delta\eta < 10^{3.25}$. For Newtonian ice (where $n = 1$), mobile lid convection occurs for $\Delta\eta < 10^4$ or $\theta < 8$. Figure 2 (top) summarizes the locations of the simulations in $Ra_1-\Delta\eta$ space. Simulations were performed using the finite element convection model CITCOM [*Moresi and Solomatov*, 1995], in a 2-D Cartesian domain with 64×64 elements. For ease of comparison between my scaling and those of previous studies, and to easily relate the behavior of the convection to the behavior of the thermal boundary layers, a temperature-dependent viscosity of form

$$\eta = \eta_0 \exp(-\gamma T) \tag{10}$$

is used, where $\gamma = \theta/\Delta T$. With this type of temperature dependence, Ra_0 is related to the more commonly used Ra_1 as $Ra_0 = Ra_1 \exp(-\theta)$. Free slip boundary conditions were used on the vertical surfaces of the domain, and constant temperature boundary conditions were used on the surface and base of the ice shell. The constant temperature boundary condition at the base of the ice shell ensures that it is forced to be in thermodynamic steady state with an underlying ocean at $T \sim T_m \sim 273$ K [*McKinnon and Barr*, 2008]. The surface temperature $T_s = 70$ K used here is appropriate for the south polar region in the absence of internal heating [*Spencer et al.*, 2006].

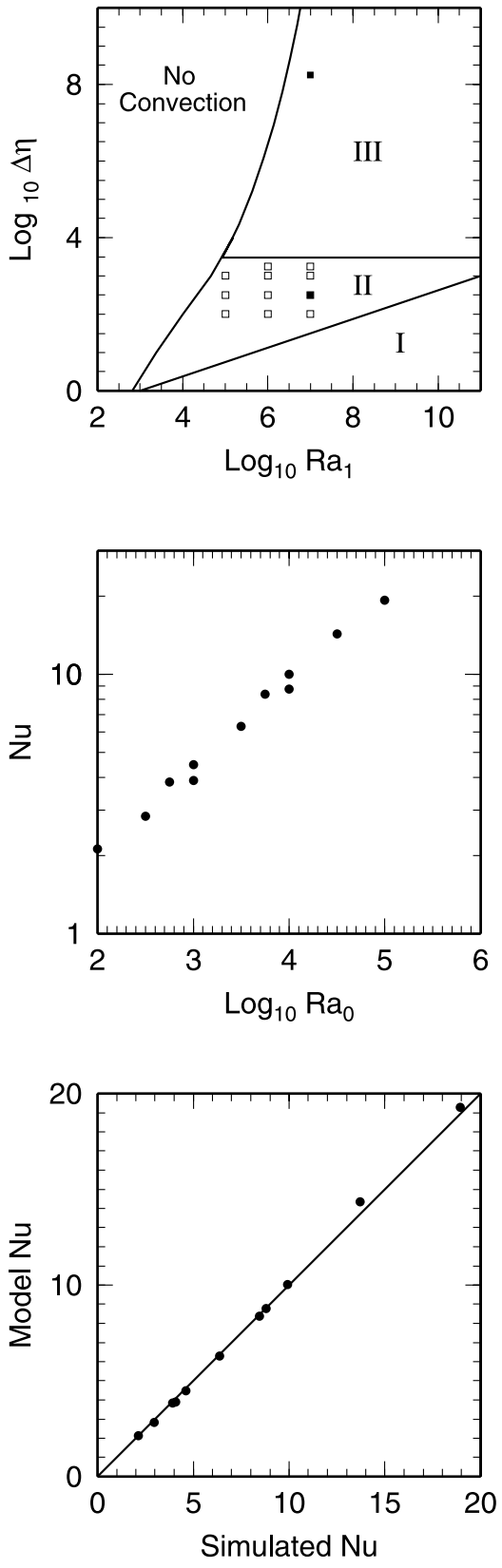

Table 1. Simulation Results for Newtonian Convection in the Mobile Lid Regime

$\Delta\eta$	Ra_1	Ra_0	v_{rms}[a]	max($\lvert v_{x,sf}\rvert$)[a]	Nu
10^2	10^5	10^3	42.6	22.3	3.89
10^2	10^6	10^4	188	136	8.87
10^2	10^7	10^5	817	788	19.3
$10^{2.5}$	10^5	$10^{2.5}$	30.4	8.60	2.83
$10^{2.5}$	10^6	$10^{3.5}$	110	22.1	6.29
$10^{2.5}$	10^7	$10^{4.5}$	609	358	14.4
10^3	10^5	10^2	21.4	3.02	2.12
10^3	10^6	10^3	110	22.1	4.48
10^3	10^7	10^4	485	143	10.0
$10^{3.25}$	10^6	$10^{2.75}$	100	13.3	3.84
$10^{3.25}$	10^7	$10^{3.75}$	440	90.3	8.32

[a]Nondimensional value.

[20] Table 1 summarizes the values of Nu obtained in the convection simulations. The majority of the simulations have $10^6 < Ra_1 < 10^7$, close to expected values for Enceladus' ice shell with melting point viscosities for ice, 10^{13} Pa s $< \eta_1 < 10^{16}$ Pa s. Simulations were run until Nu and the r.m.s. velocity were constant as a function of time; none of the solutions were time dependent, although, time-dependent behavior is expected for larger Ra_1 [*Moresi and Solomatov*, 1998] and in internally heated cases [*Solomatov*, 2004].

[21] In the mobile lid regime, if the numerical domain width is comparable to the natural wavelength of convective downwellings, free slip boundary conditions on the vertical edges of the domain can promote the formation of artificially elongated cells [*Kameyama and Ogawa*, 2000]. As a result, obtaining extremely accurate values of Nu requires running simulations in long aspect ratio domains. Table 2 summarizes Nu values for $Ra_1 = 10^6$ and $\Delta\eta$ as a function of aspect ratio for 1×1 through 8×1 domains. The values of Nu are roughly the same for aspect ratios up to 4×1, because in each of these cases, the heat is transported by a single elongated cell with downwellings at the edge of the

Figure 2. (top) Convective regime diagram for a Newtonian fluid [cf. *Solomatov*, 1995]. Typically, simulations of convection on icy satellites are performed in the stagnant lid regime (III) where large $\Delta\eta$ values lead to the development of a rigid lid of immobile ice near the surface of a convecting shell. Boxes represent locations in Ra_1 and $\Delta\eta$ parameter spaces of simulations used to constrain the coefficients in the scaling relationship between Ra and Nu in the mobile lid convective regime (II). Filled boxes represent locations in parameter space of simulations shown in Figure 1. (middle) Nu values as a function of Ra_0. (bottom) Comparison between Nu values obtained in numerical simulations and predicted by the scaling relationship (equation (8)) with $a = 0.32$ and $b = 19$.

Table 2. Dependence of Nu on Domain Aspect Ratio for $Ra_1 = 10^6$ and $\Delta\eta = 10^{2.5}$

Aspect Ratio	Nu	v_{rms}[a]	Cells
1 × 1	6.30	140	1
2 × 1	6.25	132	1
4 × 1	6.25	132	1
8 × 1	6.04	149	2

[a]Nondimensional value.

domain. The value of Nu decreases by 2% in an 8 × 1 domain because two full convection cells can be maintained. For a 50 km thick ice shell on Enceladus, an 8 × 1 aspect ratio domain would encompass 25% of the circumference of the satellite: a situation that is better simulated in a fully 3-D spherical geometry. Here, I simulate convection in a 1 × 1 domain because the measured SPT heat flux is uncertain to within a factor of ~2, so it is not necessary to know Nu to better than ~10% accuracy. If mobile lid convection appears to be consistent with the geology of the SPT, more sophisticated geometries should be used in future work to provide tighter constraints on heat flux.

[22] A fit to the $Ra - Nu$ data gives

$$Nu = 0.32 Ra_0^{1/3} \exp(\theta/19), \tag{11}$$

similar to the relationship obtained by *Moresi and Solomatov* [1998], whose simulations were performed for higher Ra than used here. The scaling is accurate to within 0.1% for low Ra, high $\Delta\eta$, and low Nu, and the accuracy decreases as Nu increases. This likely occurs because η_i is weakly dependent on Ra_0 [*Moresi and Solomatov*, 1998]; inclusion of this effect would cause the power on Ra_0 in equation (8) to change by ~10%.

3.3. Convective Heat Flux

[23] The convective heat flux is related to Ra_0 and $\Delta\eta$ as

$$F_{conv} = \frac{k\Delta T}{D} Nu = \frac{k\Delta T}{D} a Ra_0^{1/3} \exp(\theta/b), \tag{12}$$

where $a = 0.32$ and $b = 19$ (see section 3.2). Evaluating Ra_0 in terms of the physical properties of the ice shell and the thermal properties of water ice,

$$F_{conv} = 0.32 \left(\frac{\rho g \alpha \Delta T^4 k^3}{\kappa}\right)^{1/3} \frac{\exp(\theta/19)}{\eta_0^{1/3}}, \tag{13}$$

where η_0 is the effective surface viscosity of the ice shell. Similar to the stagnant lid regime, the convective heat flux is independent of the ice shell thickness, but depends on the boundary temperatures (through ΔT) and is critically dependent upon the ice rheology, through η_0 and θ. Figure 3 (right) illustrates that only a narrow range of surface viscosities, 10^{16} Pa s < η_0 < 10^{17} Pa s gives convective heat fluxes comparable to those observed by CIRS.

[24] The free parameters in F_{conv} are the basal ice viscosity, η_1, and θ, which appears explicitly in the exponential term, and implicitly in $\eta_0 = \eta_1$ $\Delta\eta = \eta_1 \exp(\theta)$. The heat flux can be expressed in terms of η_1 as

$$F = 0.32 \left(\frac{\rho g \alpha \Delta T^4 k^3}{\kappa}\right)^{1/3} \frac{\exp(\theta/19)}{\eta_1^{1/3} \exp(\theta/3)}. \tag{14}$$

Figure 3 (left) illustrates how the convective heat flux varies as a function of $\Delta\eta$ and η_1. For the highest value of $\Delta\eta = 10^{3.25}$, a basal viscosity between $\eta_1 = 10^{13}$ and 10^{14} Pa s, similar to values expected from the volume diffusion rheology with grain sizes $d \sim 0.1-1$ mm, gives F_{conv} comparable to the regional heat flux observed in the SPT. For smaller $\Delta\eta$, convection becomes more vigorous, so larger basal viscosities can give F_{conv} comparable to the values observed.

4. Tidal Heat Generation

[25] To remain thermodynamically stable, the amount of heat generated within Enceladus' ice shell from tidal dissi-

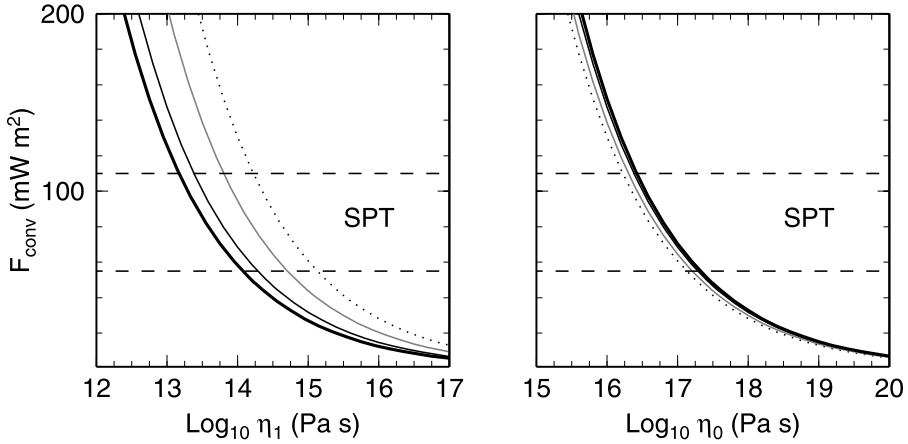

Figure 3. (left) Convective heat flux from an ice shell on Enceladus convecting in the mobile lid regime as a function of basal viscosity (η_1) for $\Delta\eta = 10^2$ (dotted), $\Delta\eta = 10^{2.5}$ (gray), $\Delta\eta = 10^3$ (thin black), and $\Delta\eta = 10^{3.25}$ (thick black). For $\Delta\eta = 10^{3.25}$, a basal viscosity between $\eta_1 = 10^{13}$ and 10^{14} Pa s gives F_{conv} comparable to the regional heat flux observed in the SPT (55 mW m^{-2} < F < 110 mW m^{-2}). For smaller $\Delta\eta$, larger basal viscosities are required to give F_{conv} close to the value observed. (right) Same as for left, but plotted as a function of the surface viscosity η_0. Only a narrow range of surface viscosities, 10^{16} Pa s < η_0 < 10^{17} Pa s give F_{conv} comparable to the observed heat flux.

Table 3. Physical and Rheological Properties of Enceladus' Interior

Layer	Parameter	Symbol	Value
Rocky Core	Radius	R_c	161 km
Rocky Core	Density	ρ_c	3500 kg m^{-3}
Rocky Core	Young's modulus	E_c	2.5×10^{11} Pa
Rocky Core	Poisson's ratio	ν_c	0.25
Ocean	Thickness	D_{ocean}	Variable
Ocean	Density	ρ_w	1000 kg m^{-3}
Ocean	P-wave velocity	$v_{p,w}$	1.45 km s^{-1}
Ice Shell	Thickness	D	Variable
Ice Shell	Density	ρ	920 kg m^{-3}
Ice Shell	Young's modulus	E_i	8×10^9 Pa
Ice Shell	Poisson's ratio	ν_i	0.325
Ice Shell	Mean ice viscosity	η	10^{14}–10^{22} Pa s

pation must approximately equal the amount of heat transported by convection. If the convective heat flux exceeds the amount of tidal heating, the interior of the satellite will cool, causing the underlying ocean to freeze [*Moore*, 2006; *Roberts and Nimmo*, 2008]. In addition to controlling the convective heat flux, the rheology of Enceladus' shell controls the height of the daily tidal deformation experienced by the satellite, by affecting its degree-2 Love numbers [*Mullen*, 2006; *Nimmo et al.*, 2007]. Previous work shows that the volumetric tidal dissipation rates in an ice shell in the stagnant lid regime are significantly smaller than the convective heat flux [*Roberts and Nimmo*, 2008]. If the ice shell had a rheology governed purely by volume diffusion, the presence of the high-viscosity stagnant lid would suppress tidal deformation and limit the amount of tidal dissipation [*Moore*, 2006; *Roberts and Nimmo*, 2008]. However, this balance has not been explored in the small $\Delta\eta$ regime. Here, tidal dissipation within the shell is modeled as viscous dissipation in a Maxwell viscoelastic solid, and related to the tidal potential from Saturn using the h_2 Love number of a model Enceladus with a floating ice shell. The surface heat flux from tidal dissipation is compared to the convective heat flux and the observed heat flux from CIRS.

[26] The heating rate per unit mass within the ice shell due to viscous dissipation driven by diurnal tidal deformation is [*Ojakangas and Stevenson*, 1989; *Showman and Han*, 2004]

$$H = \frac{\dot{\varepsilon}^2 \eta}{2\rho\left(1 + \left(\frac{\omega\eta}{\mu}\right)^2\right)}, \tag{15}$$

where

$$\dot{\varepsilon} \sim 3 \times 10^{-9} (h_2) \text{s}^{-1} \tag{16}$$

is the tidal strain rate [*Nimmo et al.*, 2007], h_2 is the Love number relating diurnal tidal deformation to the tidal force on Enceladus from Saturn, $\omega = 2\pi/T_E = 5.308 \times 10^{-5}$ s^{-1} is Enceladus' orbital frequency, $T_E = 1.37$ days is Enceladus' orbital period, and $\mu = 3.5 \times 10^9$ Pa is the shear modulus of ice. Similar to section 2, here, I make the approximation that tidal dissipation is uniformly distributed within an ice shell that is thin compared to the radius of the satellite, with an average heating rate given by equation (15) with η evaluated at the viscosity in the well-mixed convective interior of the ice shell. In this case, the surface heat flux from tidal dissipation is

$$F_{\text{tidal}} = \rho H D = \frac{\dot{\varepsilon}^2 \eta_i D}{2\left(1 + \left(\frac{\omega\eta_i}{\mu}\right)^2\right)}. \tag{17}$$

[27] The strain rate in Enceladus' ice shell is calculated using h_2 for a satellite consisting of an elastic rocky core, a subsurface liquid water ocean, and a viscoelastic ice shell (J. Wahr et al., Modeling stresses on satellites due to nonsynchronous rotation and orbital eccentricity using gravitational potential theory, submitted to Icarus, 2008). In the simulations of mobile lid convection, the viscosity in the ice shell is $\eta_i \approx \eta_0 \exp(\theta/2)$ (see, e.g., Figure 1 (bottom)). Because the ice viscosity is approximately constant, Love numbers of the satellite are determined using a single layer of ice of variable thickness with a range of η values appropriate for the well-mixed interiors of ice shells convecting in the mobile lid regime.

[28] Values of h_2 for the model satellite due to the applied tidal potential from Saturn are calculated using the correspondence principle [*Sabadini et al.*, 1982], using the SatStress software package (J. Wahr et al., submitted manuscript, 2008). This approach has been used to study tidal heating in both rocky and icy satellites including Io, Europa, and Enceladus [*Segatz et al.*, 1988; *Ross and Schubert*, 1989; *Moore and Schubert*, 2000; *Wahr et al.*, 2006; *Moore*, 2006; *Nimmo et al.*, 2007]. Mechanical and rheological parameters used for each layer of the satellite are summarized in Table 3. Using the same mechanical and rheological properties of ice, and the same physical structure for the interior of Enceladus, my values of h_2 match those reported by *Nimmo et al.* [2007] to 10%.

[29] Figure 4 (top) illustrates how h_2 varies as a function of ice shell viscosity and thickness. For an ice shell 30 km thick, h_2 decreases from 0.18 to 0.03 as the viscosity in the ice shell is increased from 10^{13} to 10^{16} Pa s. The maximum $h_2 \sim 0.65$ occurs for the thinnest ice shell, $D = 8$ km and the lowest viscosity, $\eta = 10^{13}$ Pa s. Figure 4 (bottom) illustrates how the global mean diurnal tidal strain rate $\dot{\varepsilon} \approx 3 \times 10^{-9}\ h_2$ s^{-1} varies as a function of ice shell thickness and viscosity. Strain rates vary from $\dot{\varepsilon} \sim 3 \times 10^{-10}$ to 3×10^{-11} s^{-1} and are maximized in thin, low-viscosity ice shells.

[30] Figure 5 summarizes a comparison between F_{tidal} and F_{conv} a function of the surface viscosity η_0. For a broad range of plausible ice shell viscosities, the tidal heat generation falls short of the convective heat flux, in most cases, by a factor of ~10 or more. The amount of tidal dissipation calculated here represents an upper limit on heat generation in a mobile lid shell. Because mobile lid behavior of the ice shell is confined within Enceladus' SPT and is not occurring everywhere on Enceladus, the remainder of its ice shell may have a high effective near-surface viscosity. However, the tidal deformation model described above assumes a radially symmetric viscosity structure and thus, that Enceladus' ice shell has a low near-surface viscosity everywhere. The values of h_2 calculated using the globally low viscosity assumed here are therefore upper limits. In a more realistic model, tidal deformation in the SPT might be limited by the high viscosity of the remainder of Enceladus' lithosphere and may be much lower than

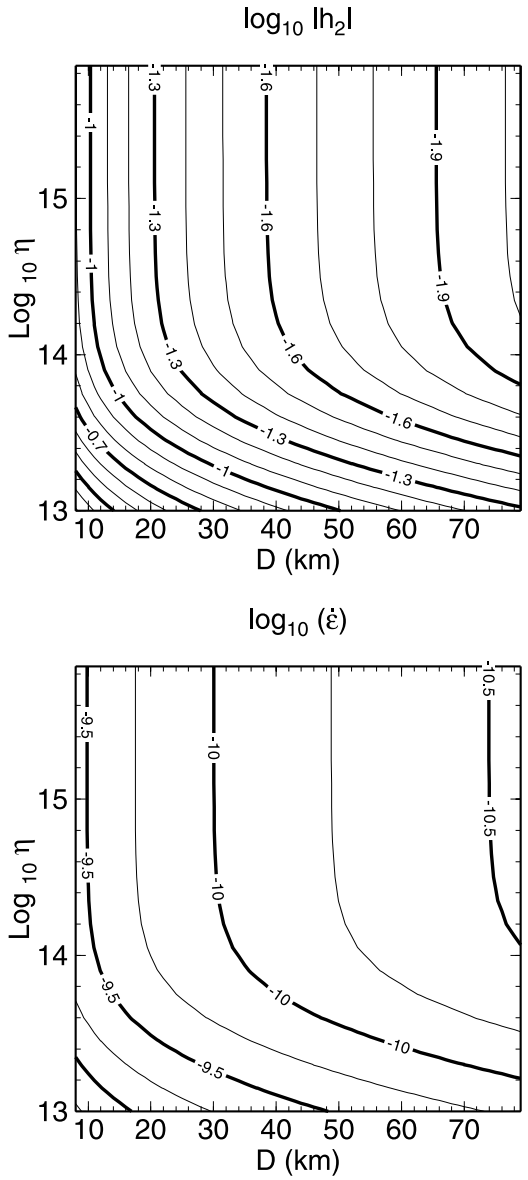

Figure 4. (top) Contours of $\log_{10}(|h_2|)$, the magnitude of degree 2 Love number h, as a function of ice shell thickness and viscosity. The amount of diurnal deformation on Enceladus that gives rise to tidal dissipation in the ice shell is proportional to h_2. (bottom) Contours of $\log_{10}(\dot{\varepsilon})$ (in units of s^{-1}), the global, time-averaged diurnal tidal strain rate in a floating ice shell on Enceladus, as a function of ice shell thickness and viscosity. Diurnal deformation and strain rates are large in thin ice shells and in shells with high viscosity.

estimates in Figure 5. It is also possible that tidal deformation could become concentrated within a low-viscosity zone at the south pole [*Moore*, 2001]. Further work to determine how tidal strain is partitioned in an ice shell with a heterogeneous viscosity structure is required to properly evaluate the balance between tidal heating and convection.

5. Requirements for Mobile Lid Behavior

[31] The presence of solid state convection in Enceladus' ice shell is not a foregone conclusion [*Barr and McKinnon*, 2007]. For convection to occur, the Rayleigh number in the ice shell must exceed a critical value. The critical Rayleigh number for convection in a basally heated fluid layer convecting in the moderate viscosity contrast regime has been constrained by *Stengel et al.* [1982] using linear stability analysis and laboratory experiments. Unlike in the stagnant lid regime, there is no clear relationship between the critical Rayleigh number and $\Delta\eta$ for moderate $\Delta\eta$. Table 4 summarizes the values of critical Rayleigh number for convection in a Newtonian fluid as a function of $\Delta\eta$ obtained by *Stengel et al.* [1982]. For mobile lid convection to occur, $Ra_1 > Ra_{cr,1}$. Evaluating Ra_1 in terms of the properties of the ice shell,

$$Ra_1 = \frac{\rho g \alpha \Delta T D^3}{\kappa \eta_1 \Delta}, \tag{18}$$

and solving for the critical ice shell thickness where convection is possible,

$$D > \left(\frac{\eta_0 Ra_{cr,1}\kappa}{\rho g \alpha \Delta T \Delta\eta}\right)^{1/3}. \tag{19}$$

For $\Delta\eta = 10^3$, in an ice shell with a heat flux comparable to that measured by CIRS, $\eta_0 \approx 10^{16}$ Pa s, which implies that convection can occur if $D > 5$ km. The critical Rayleigh number criterion is easily achieved even in a thin ice shell on Enceladus in the mobile lid regime. However, if convection itself (perhaps coupled with tides) is required to damage the near-surface ice and induce mobile lid behavior, convection may have to be initially triggered in an ice shell with a high effective viscosity contrast. In this case, the basal viscosity of the shell must be relatively low, $\sim 10^{13}$–10^{14} Pa s, and the ice shell relatively thick, $D \approx$ 100 km, for convection to start [*Barr and McKinnon*, 2007].

[32] So far, I have used the criterion that mobile lid behavior can occur in Enceladus' ice shell if $\Delta\eta < 10^4$. The most straightforward method of lowering the effective viscosity contrast in the ice shell is to suppose that the effective viscosity of the cold near-surface ice is limited by the finite yield stress of ice. Recently, *Solomatov* [2004] has developed a general criterion for the critical yield strength for lid mobilization on the basis of the rheology of the convecting layer. For convection to occur in the mobile lid regime, stresses built up in the lithosphere have to be comparable to the yield strength of the lithosphere [*Solomatov*, 2004]

$$\sigma_{Y,cr} \lesssim 13 \frac{\alpha \rho g}{\Delta T}\left(\frac{RT_i^2}{Q_v^*}\right)^2 l_h, \tag{20}$$

where $T_i \sim 273$ K is the characteristic temperature beneath the upper thermal boundary layer, and $l_h \sim D$ is the horizontal length scale over which stress accumulates in the lithosphere [*Solomatov*, 2004], which is comparable to the width of convective upwellings. For parameters appropriate to convection in a 30 km thick ice shell on Enceladus, where deformation is accommodated by volume diffusion, $\sigma_{Y,cr} \sim 3 \times 10^{-3}$ MPa.

[33] Field characterization of fracture in the Ross Ice Shelf suggest that the yield stress of ice is ~0.1 MPa

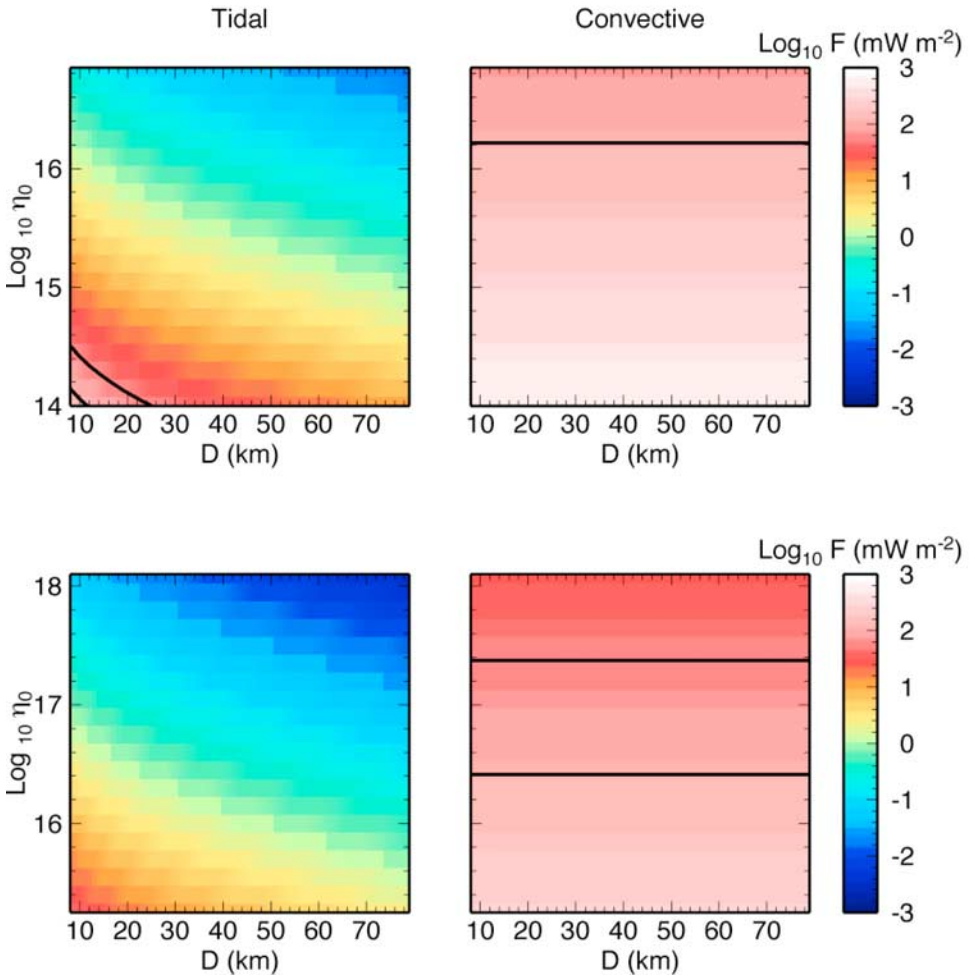

Figure 5. Surface heat flux from (left) tidal heating in a constant viscosity ice shell and (right) mobile lid convection, as a function of surface viscosity and ice shell thickness for $\Delta\eta = 10^2$ (top row) and $\Delta\eta = 10^{3.25}$. Red values and contours show heat fluxes close to the SPT heat flux observed by CIRS. Regardless of the viscosity contrast across the ice shell, tidal heat generation is a factor of ~10 lower than the heat transported across the ice shell by mobile lid convection.

[*Kehle*, 1964; *Showman and Han*, 2005], much larger than the critical yield stress for mobile lid convection. Terrestrial field estimates for σ_Y may not be directly applicable to the surfaces of icy satellites, because measurements are usually acquired at ambient temperatures ~240–273 K. The microphysical processes responsible for fracture in macroscopic terrestrial ice bodies (e.g., grain boundary sliding and dislocation pileups [*Frost*, 2001]) are thermally driven [*Sinha*, 1991], and are not likely to be responsible for fracture in ice with temperatures relevant to Enceladus' lithosphere, $T \sim 70$–180 K.

[34] Estimates of the yield strength of Europa's lithosphere, which may be more similar in terms of temperature and microtexture to the lithosphere of Enceladus than terrestrial ice, range from ~0.01–0.1 MPa. The lower bound on yield stress arises from the observation that cycloidal ridges on Europa propagate in response to daily tidal stresses, which have magnitudes ~0.01 MPa assuming a floating ice shell [*Hoppa et al.*, 1999]. It is possible, however, that stresses twice as high are required to initiate cycloids on Europa [*Hurford et al.*, 2007b], and this larger initiation stress may be more relevant to lithospheric fracturing than the lower propagation stress. If Europa's bands form in a style similar to terrestrial midocean ridge spreading [*Prockter et al.*, 2002], a lithospheric yield strength of 0.4 to 2 MPa is consistent with the width of fault blocks flanking the band's central trough [*Stempel et al.*, 2005].

[35] It has been suggested that plume activity in the SPT is driven in part by opening and closing of portions of the tiger stripes because of the diurnal tidal stresses [*Hurford et al.*, 2007a]. If that were the case, diurnal stresses on Enceladus, similar to Europa, may be able to drive at least superficial lithospheric cracking. Using the values of h_2

Table 4. Critical Rayleigh Number for Mobile Lid Convection After *Stengel et al.* [1982]

$\Delta\eta$	$Ra_{1,cr}$
10^2	1.01×10^4
$10^{2.5}$	2.12×10^4
10^3	4.70×10^4
$10^{3.25}$	6.41×10^4

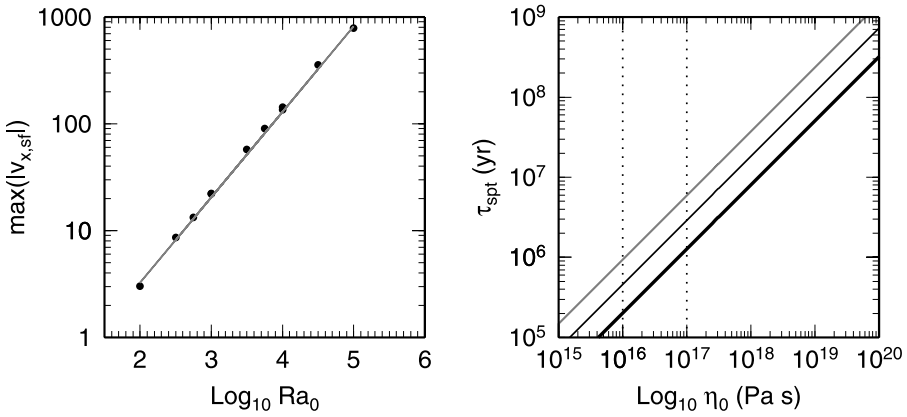

Figure 6. (left) Maximum horizontal velocity max($|v_{x,sf}|$) of surface material as a function of Ra_0 from numerical simulations (dots). Gray line shows the fit to the data using equation (23). (right) Predicted age of the south polar terrain on Enceladus τ_{spt} if mobile lid convection controls lithospheric recycling. Predicted surface ages increase as the effective viscosity of the surface ice (η_0) increases and decrease as the thickness of the ice shell is increased from D = 30 (gray) to D = 50 km (thin black) and D = 90 km close to the thickest possible ice shell on a differentiated Enceladus. Dotted lines show the range of surface viscosities required to give convective heat fluxes comparable to the regional heat flux observed at the SPT by Cassini CIRS, which constrain the surface age to be between 0.2 and 7 Ma, depending on the ice shell thickness.

Love number calculated in section 4, this suggests yield stresses for Enceladus' lithosphere of less than ~500 (h_2) kPa, or ~5–50 kPa for $h_2 \sim 0.01$ to 0.1, depending on the properties of the near-surface ice.

[36] Because Enceladus is a small body with relatively low gravity, and its convection is driven by small temperature fluctuations, the yield stress required for mobile lid convection is extremely low. The required yield stress is seemingly a factor of ~10 lower than estimates of the yield stress derived from models of Europa's surface geology, and a factor of ~1000 lower than yield strength estimates from terrestrial ice sheets. It should be noted that a similar situation occurs on Earth, where the yield stress of rock measured in laboratory contexts is a factor of ~10 higher than the critical yield stress for the initiation of subduction [*Solomatov*, 2004]. On Earth, one can appeal to chemical variations such as the presence of water [*Solomatov*, 2004] and/or semibrittle behavior of the lithosphere due to microcracking and faulting [*Kohlstedt et al.*, 1995; *Tackley*, 2000; *Bercovici*, 2003] to mobilize the lid. On Enceladus, the presence of the tiger stripes suggest that tidal stresses alone, or acting in concert with convective stresses, may be sufficient to fracture the near-surface ice. Because tidal strain and strain rates are maximized on Enceladus' poles [*Ojakangas and Stevenson*, 1989], the likelihood of tidally induced lithospheric fracture is highest at this location. Improved knowledge of the friction and failure of cold ice and the interaction between convective and tidal stresses in icy satellite lithospheres can shed light upon the likelihood of mobile lid convection on icy bodies.

6. Geological Consequences

[37] As the name implies, convection in the mobile lid regime leads to substantial horizontal velocities of near-surface ice. If mobile lid convection is responsible for lithospheric recycling and surface deformation at the SPT, the SPT should have a younger surface than the rest of Enceladus, and the age of the surface should be related to the horizontal velocity of the surface ice. The horizontal velocities are related to the convective heat flux through Ra_0 and η_0. Rapid extension or spreading in the SPT must be balanced by material loss at its flanks, so understanding the processes by which extension/spreading in the SPT is accommodated by the regional geology is a key to evaluating the plausibility of mobile lid convection. Here I describe how these geological consequences provide a means by which the mobile lid convection hypothesis can be tested using Cassini data.

6.1. Relationship Between SPT Age and Surface Viscosity

[38] The characteristic convective velocities in the upper boundary layer, v_0, are inversely proportional to the boundary layer thickness, δ_0 [*Solomatov*, 1995]

$$v_0 \sim \left(\frac{D}{\delta_0}\right)^2 \frac{\kappa}{D} \sim Ra_0^{2/3} \frac{\kappa}{D}. \tag{21}$$

Note that nondimensional velocities such as those reported in Tables 1 and 2 may be expressed in meters per second by multiplying by κ/D, where D is the ice shell thickness. Because $\delta_0 \sim Ra_0^{-1/3}$, the near-surface velocity scales with the surface Rayleigh number as $v_0 \propto Ra_0^{2/3}$. Nondimensional values of the maximum horizontal velocity of surface ice, max($|v_{x,sf}|$), obtained in each of the mobile lid simulations are summarized in Table 1. The maximum horizontal velocity scales as

$$\max\left(|v_{x,sf}|\right) = 0.08 Ra_0^{0.8} \frac{\kappa}{D}. \tag{22}$$

Figure 6 illustrates the dependence of max($|v_{x,sf}|$) on Ra_0 and shows the fit to the values obtained in the numerical

simulations. The dependence of surface velocity on Ra_0 implies that surface velocities for the ice shell will depend on η_0 and the shell's thermal and physical parameters,

$$\max\left(|v_{x,\mathrm{sf}}|\right) = 0.08\frac{\kappa}{D}\left(\frac{\rho g\alpha\Delta T D^3}{\kappa}\right)^{0.8}\frac{1}{\eta_0^{0.8}}. \quad (23)$$

Unlike the convective heat flux, the surface velocity is dependent on the ice shell thickness D: even if the fit had yielded an exact $Ra_0^{2/3}$ dependence, the surface velocity would still depend on D. Evaluating the velocity using thermal and physical parameters appropriate for Enceladus' ice shell,

$$\max\left(|v_{x,\mathrm{sf}}|\right) = 25\,\mathrm{mm\,a^{-1}}\left(\frac{10^{17}\mathrm{Pa\,s}}{\eta_0}\right)^{0.8}\left(\frac{D}{30\,\mathrm{km}}\right)^{1.4}, \quad (24)$$

comparable to spreading rates on midocean ridges on Earth [e.g., *Turcotte and Schubert*, 1982] and comparable to estimates of the spreading rates on band-type features on Europa [*Stempel et al.*, 2005].

[39] For a circular SPT with an area 70,000 km^2 [*Porco et al.*, 2006], the equivalent radius of the region is $R_{\mathrm{spt}} \sim$ 150 km. If mobile lid convection is the driving force for resurfacing, the age of the surface is related to the shell thickness and viscosity as

$$\tau_{\mathrm{spt}} \sim \frac{R_{\mathrm{spt}}}{\max\left(|v_{x,\mathrm{sf}}|\right)} \sim 6\mathrm{Ma}\left(\frac{\eta_0}{10^{17}\mathrm{Pa\,s}}\right)^{0.8}\left(\frac{30\,\mathrm{km}}{D}\right)^{1.4}. \quad (25)$$

Figure 6 (right) illustrates how the predicted age of the SPT varies as a function of η_0 and D. For the range of surface viscosities that give F_{conv} close to the heat flux observed by CIRS, the predicted age of the SPT is between 0.2 and 7 Ma, depending on the ice shell thickness. This is consistent with the 0.5 Ma age inferred from the lack of craters with diameter greater than 1 km [*Porco et al.*, 2006], but more detailed studies are needed to place tighter constraints on the cratering statistics. Ages significantly longer than 7 Ma require convection that is too sluggish to give the observed heat flux; conversely, ages much less than 0.2 Ma imply $F_{\mathrm{conv}} > F$.

6.2. Lithospheric Loss at Cusps

[40] Regional extension or spreading at the SPT driven by mobile lid convection must be balanced by the loss of material at the flanks of the terrain. On Enceladus, the SPT seems to be bounded by a series of arcuate features, which join at cusps. Folding at the cusps suggest that they may be sites of convergent tectonic activity [*Helfenstein et al.*, 2006] and are a natural location to accommodate the regional extension or spreading predicted to occur in mobile lid convection.

[41] Unfortunately, the processes by which icy satellites accommodate compressional deformation and lose surface material are not well understood. On terrestrial planets, crustal loss occurs by subduction. Although it is tempting to appeal to subduction or a subduction-like process on Enceladus, it is not clear how local density differences of the magnitude required for lithospheric fracture and foundering might be created. One way of generating negative buoyancy within an ice shell is to generate local melting, but whether the melt simply drains through the ice shell or is retained to create local negative buoyancy depends on the poorly understood details of how melt drains within satellite ice shells.

[42] On terrestrial planets, crustal loss can also occur beneath continents where the thickened, cold, lithosphere can become gravitationally unstable and sink into the mantle [e.g., *Molnar et al.*, 1998]. Similar processes have been suggested to balance the seemingly ubiquitous lithospheric extension on Europa. For example, *Prockter and Pappalardo* [2000] have identified a set of long-wavelength, low-amplitude folds on the surface of Europa which could represent locations of local thickening of the lithosphere and crustal loss. On Enceladus, the folded terrain within the cusps could represent sites of locally thickened lithosphere and cold, negatively buoyant ice dripping into the underlying warm convecting ice shell. Characterization of the long-wavelength topography within the SPT and at its margins may be able to shed light on the processes by which regional extension is accommodated.

7. Discussion

[43] The discovery of the warm cryovolcanically and possibly tectonically active south polar region of Enceladus provides a unique opportunity to understand the relationship between tidal dissipation, heat transport, and resurfacing on icy satellites. The high regional heat flux at the SPT, F = 55 to 110 mW m^{-2}, is a factor of $\sim$3–4 higher than predicted by prior studies of stagnant lid convection on Enceladus [*Barr and McKinnon*, 2007; *Roberts and Nimmo*, 2008]. If Enceladus' surface ice has a viscosity as high as values predicted by the theoretically constrained volume diffusion rheology, convective heat transport is limited to $\sim$15–30 mW m^{-2}, and the amount of tidal dissipation within the ice shell falls short of the observed heat flux, as well [*Roberts and Nimmo*, 2008].

[44] Here, I have proposed that Enceladus' south polar region is a location where the near-surface ice is relatively weak, which permits convective fluid motions to reach closer to the surface and drive lithospheric deformation. The effects of a weak brittle lithosphere are mimicked in the framework of a purely viscous convection model by limiting the effective viscosity of the near-surface ice. If the ratio between the effective surface viscosity and basal viscosity of the ice shell is less than 10^4, Enceladus' SPT convects in the so-called "mobile lid" regime of convective behavior, which is characterized by large heat fluxes.

[45] Heat fluxes comparable to those observed by CIRS are possible if the effective viscosity of the surface ice is $\eta_0 \sim 10^{16}$ to 10^{17} Pa s. Such low effective viscosities near the surface of the ice shell permit the near-surface ice to be mobilized by the underlying convection, which may drive rapid resurfacing in the SPT. If mobile lid convection is occurring, the age of the SPT should be $\tau_{\mathrm{spt}} \sim O(0.1-10)$ Ma. A paucity of craters larger than 1 km on the south polar terrain suggests that its surface is less than 0.5 Ma old [*Porco et al.*, 2006], which is consistent with mobile lid behavior. If mobile lid convection is occurring in the SPT, the lithospheric spreading associated with convective

upwellings must be balanced by loss of surface ice at the margins of the region. This would be consistent with the presence of convergent tectonics at the margins of the SPT [*Helfenstein et al.*, 2006]. Folded terrain observed at the cusps between cycloidal arcs that bound the SPT may represent locations of thickened lithosphere where cold near surface ice pushed into the cusps drips down into the underlying convecting ice shell in the style of sublithospheric instabilities beneath terrestrial continents.

[46] The amount of tidal heating generated in a mobile lid ice shell falls short of the amount of heat transported by mobile lid convection. At face value, this suggests that mobile lid convection might be a transient phenomenon because the efficient convective heat transport in the mobile lid regime would cause Enceladus' ocean to freeze [*Roberts and Nimmo*, 2008]. The model used to calculate tidal dissipation assumes that Enceladus has a radially symmetric viscosity structure. A more realistic model would consider the SPT to be a low-viscosity region embedded in an ice shell with an otherwise high viscosity. If such a structure allowed tidal deformation to become concentrated within the SPT, it may be able to generate higher local heating rates than calculated here [cf. *Moore*, 2001] and perhaps permit an equilibrium between tidal dissipation and convection. Another possibility is that Newtonian volume diffusion does not accommodate diurnal tidal strain in Enceladus' ice shell. If another processes, such as grain boundary sliding, accommodated tidal deformation, the effective viscosity of the ice shell over tidal timescales would be different from the effective viscosity over convective timescales [*McKinnon*, 1999]. Very little is known about the microphysical processes responsible for attenuation in water ice that is being cyclically flexed at frequencies appropriate to tidal deformation on Enceladus. Such information is critically needed to help clarify the relationship between tidal flexing and the activity at the SPT.

[47] It has been previously suggested that shear heating due to strike slip motion along fault zones within the centers of the tiger stripes provide a substantial amount of heat to the total observed heat flux at the SPT [*Nimmo et al.*, 2007]. Such a heat source is compatible with the presence of mobile lid convection, and indeed, the two processes acting in concert may be able to provide a total heat flux comparable to that observed by CIRS. Observations of the heat flux in regions of the SPT away from the tiger stripes may shed light upon how tidal dissipation in the region is partitioned between shear heating and viscous dissipation in the underlying ice shell. In addition, although a heat source representative of ridges was not included as part of the convection simulations here, the interaction between ridge heating and mobile lid convection may be a promising avenue of future work.

[48] **Acknowledgments.** This work is supported by NASA Cassini Data Analysis Grant NNX07AE80G. The author thanks G. W. Patterson and V. S. Solomatov for useful discussions and R. M. Canup for helpful feedback on the original manuscript. The author also thanks J. H. Roberts, F. Nimmo, and an anonymous reviewer for useful comments. This work has benefitted significantly from previous work and discussion with W. B. McKinnon.

References

Barr, A. C., and W. B. McKinnon (2007), Convection in Enceladus' ice shell: Conditions for initiation, *Geophys. Res. Lett.*, *34*, L09202, doi:10.1029/2006GL028799.

Bercovici, D. (2003), The generation of plate tectonics from mantle convection, *Earth Planet. Sci. Lett.*, *205*, 107–121.

Booker, J. R. (1976), Thermal convection with strongly temperature-dependent viscosity, *J. Fluid Mech.*, *76*, 741–754.

Frost, H. J. (2001), Mechanisms of crack nucleation in ice, *Eng. Fract. Mech.*, *68*, 1823–1837.

Goldsby, D. L., and D. L. Kohlstedt (2001), Superplastic deformation of ice: Experimental observations, *J. Geophys. Res.*, *106*, 11,017–11,030.

Goodman, D. J., H. J. Frost, and M. F. Ashby (1981), The plasticity of polycrystalline ice, *Philos. Mag. A*, *43*, 665–695.

Helfenstein, P., et al. (2006), Patterns of fracture and tectonic convergence near the south pole of Enceladus, *Lunar Planet. Sci.*, *XVII*, abstract 2182.

Hoppa, G. V., B. R. Tufts, R. Greenberg, and P. E. Geissler (1999), Formation of cycloidal features on Europa, *Science*, *285*, 1899–1902.

Hurford, T. A., P. Helfenstein, G. V. Hoppa, R. Greenberg, and B. G. Bills (2007a), Eruptions arising from tidally controlled periodic openings of rifts on Enceladus, *Nature*, *447*, 292–294, doi:10.1038/nature05821.

Hurford, T. A., A. R. Sarid, and R. Greenberg (2007b), Cycloidal cracks on Europa: Improved modeling and non-synchronous rotation implications, *Icarus*, *186*, 218–233, doi:10.1016/j.icarus.2006.08.026.

Kameyama, M., and G. Ogawa (2000), Transitions in thermal convection with strongly temperature-dependent viscosity in a wide box, *Earth Planet. Sci. Lett.*, *180*, 355–367.

Kehle, R. O. (1964), Deformation of the Ross Ice Shelf, *Geol. Soc. Am. Bull.*, *75*, 259–286.

Kirk, R. L., and D. J. Stevenson (1987), Thermal evolution of a differentiated Ganymede and implications for surface features, *Icarus*, *69*, 91–134.

Kohlstedt, D. L., B. Evans, and S. J. Mackwell (1995), Strength of the lithosphere: Constraints imposed by laboratory experiments, *J. Geophys. Res.*, *100*, 17,587–17,602.

McKinnon, W. B. (1999), Convective instability in Europa's floating ice shell, *Geophys. Res. Lett.*, *26*, 951–954.

McKinnon, W. B. (2006), On convection in ice I shells of outer solar system bodies, with specific application to Callisto, *Icarus*, *183*, 435–450.

McKinnon, W. B., and A. C. Barr (2008), On the stability of an ocean within Enceladus, *Lunar Planet. Sci.*, *XXXIX*, abstract 2517.

Molnar, P., G. A. Houseman, and C. P. Conrad (1998), Rayleigh-Taylor instability and convective thinning of mechanically thickened lithosphere: Effects of non-linear viscosity decreasing exponentially with depth and of horizontal shortening of the layer, *Geophys. J. Int.*, *133*, 568–584.

Moore, W. B. (2001), Coupling tidal dissipation and convection, *Bull. Am. Astron. Soc.*, *33*, 1106.

Moore, W. B. (2006), Thermal equilibrium in Europa's ice shell, *Icarus*, *180*, 141–146, doi:10.1016/j.icarus.2005.09.005.

Moore, W. B., and G. Schubert (2000), The tidal response of Europa, *Icarus*, *147*, 317–319.

Moresi, L.-N., and V. S. Solomatov (1995), Numerical investigation of 2-D convection with extremely large viscosity variations, *Phys. Fluids*, *7*, 2154–2162.

Moresi, L.-N., and V. S. Solomatov (1998), Mantle convection with a brittle lithosphere: thoughts on the global tectonic styles of Earth and Venus, *Geophys. J. Int.*, *133*, 669–682.

Mullen, M. E. (2006), Visco-elastic surface stresses on Europa, Honors Thesis, Univ. of Colo., Boulder, Colo.

Nimmo, F., J. R. Spencer, R. T. Pappalardo, and M. E. Mullen (2007), Shear heating as the origin of plumes and heat flux on Enceladus, *Nature*, *447*, 289–291.

Ojakangas, G. W., and D. J. Stevenson (1989), Thermal state of an ice shell on Europa, *Icarus*, *81*, 220–241.

Olson, P., and G. M. Corcos (1980), A boundary layer model for mantle convection with surface plates, *Geophys. J. R. Astron. Soc.*, *62*, 195–219.

Pappalardo, R. T., et al. (1998), Geological evidence for solid-state convection in Europa's ice shell, *Nature*, *391*, 365–368.

Porco, C. C., et al. (2006), Cassini observes the active south pole of Enceladus, *Science*, *311*, 1393–1401, doi:10.1126/science.1123013.

Prockter, L. M., and R. T. Pappalardo (2000), Folds on Europa: Implications for crustal cycling and accommodation of extension, *Science*, *289*, 941–944.

Prockter, L. M., J. W. Head, R. T. Pappalardo, R. J. Sullivan, A. E. Clifton, B. Giese, R. Wagner, and G. Neukum (2002), Morphology of Europan bands at high resolution: A mid-ocean ridge-type rift mechanism, *J. Geophys. Res.*, *107*(E5), 5028, doi:10.1029/2000JE001458.

Ratcliff, J. T., P. J. Tackley, G. Schubert, and A. Zebib (1997), Transitions in thermal convection with strongly variable viscosity, *Phys. Earth. Planet. Inter.*, *102*, 201–212.

Roberts, J. H., and F. Nimmo (2008), Tidal heating and the long-term stability of a subsurface ocean on Enceladus, *Icarus*, *194*, 675–689, doi:10.1016/j.icarus.2007.11.010.

Ross, M., and G. Schubert (1989), Viscoelastic models of tidal heating in Enceladus, *Icarus*, *78*, 90–101.

Sabadini, R., D. A. Yuen, and E. Boschi (1982), Polar wandering and the forced responses of a rotating, multilayered, viscoelastic planet, *J. Geophys. Res.*, *87*, 2885–2903.

Schubert, G., D. L. Turcotte, and P. Olson (2001), Mantle Convection in the Earth and Planets, Cambridge Univ. Press, New York.

Schubert, G., J. D. Anderson, B. J. Travis, and J. Palguta (2007), Enceladus: Present internal structure and differentiation by early and long-term radiogenic heating, *Icarus*, *188*, 345–355, doi:10.1016/j.icarus.2006.12.012.

Segatz, M., T. Spohn, M. N. Ross, and G. Schubert (1988), Tidal dissipation, surface heat flow, and figure of viscoelastic models of Io, *Icarus*, *75*, 187–206.

Showman, A. P., and L. Han (2004), Numerical simulations of c convection in Europa's ice shell: Implications for surface features, *J. Geophys. Res.*, E01010, doi:10.1029/2003JE002103.

Showman, A. P., and L. Han (2005), Effects of plasticity on convection in an ice shell: Implications for Europa, *Icarus*, *177*, 425–437, doi:10.1016/j.icarus.2005.02.020.

Sinha, N. K. (1991), Kinetics of microcracking and dilatation in polycrystalline ice, in *Ice-Structure Interaction: IUTAM-IAHR Symposium, St. John's, Newfoundland, Canada*, edited by S. Jones et al., pp. 69–87, Springer-Verlag, Heidelberg, Germany.

Solomatov, V. S. (1995), Scaling of temperature- and stress-dependent viscosity convection, *Phys. Fluids*, *7*, 266–274.

Solomatov, V. S. (2004), Initiation of subduction by small-scale convection, *J. Geophys. Res.*, *109*, B01412, doi:10.1029/2003JB002628.

Solomatov, V. S., and L.-N. Moresi (2000), Scaling of time-dependent stagnant lid convection: Application to small-scale convection on Earth and other terrestrial planets, *J. Geophys. Res.*, *105*, 21,795–21,818.

Spencer, J. R., et al. (2006), Cassini encounters Enceladus: Background and the discovery of a south polar hot spot, *Science*, *311*, 1401–1405.

Stempel, M. M., A. C. Barr, and R. T. Pappalardo (2005), Model constraints on the opening rates of bands on Europa, *Icarus*, *177*, 297–304.

Stengel, K. C., D. C. Oliver, and J. R. Booker (1982), Onset of convection in a variable viscosity fluid, *J. Fluid Mech.*, *120*, 411–431.

Tackley, P. J. (2000), Mantle convection and plate tectonics: Toward an integrated physical and chemical theory, *Science*, *288*, 2002–2007.

Tobie, G., G. Choblet, and C. Sotin (2003), Tidally heated convection: Constraints on Europa's ice shell thickness, *J. Geophys. Res.*, *108*(E11), 5124, doi:10.1029/2003JE002099.

Turcotte, D. L., and G. Schubert (1982), Geodynamics: Applications of Continuum Physics to Geological Problems, John Wiley, New York.

Wahr, J. M., M. T. Zuber, D. E. Smith, and J. I. Lunine (2006), Tides on Europa, and the thickness of Europa's icy shell, *J. Geophys. Res.*, *111*, E12005, doi:10.1029/2006JE002729.

A. C. Barr, Department of Space Studies, Southwest Research Institute, 1050 Walnut Street, Suite 300, Boulder, CO 80302, USA. (amy@boulder.swri.edu)